Eleventh International Conference on CFD in the Minerals and Process Industries
CSIRO, Melbourne, Australia
7-9 December 2015

CFD FLUID FLOW MODELLING IN AMD LIME NEUTRALISATION TANKS: IDENTIFYING THE FLOW CHARACTERISTICS THAT FACILITATE SCALE FORMATION

Elyse KENNY[1*], Sara COUPERTHWAITE[1] and Graeme MILLAR[1]

[1]School of Chemistry, Physics and Mechanical Engineering, Faculty of Science and Technology , Queensland University of Technology , Brisbane , Queensland , Australia
*Corresponding author, E-mail address: elyse.kenny@hdr.qut.edu.au

ABSTRACT

Acid Mine Drainage (AMD) is a common problem observed at abandoned mine sites, and occurs when sulphide minerals are exposed to air and water that form sulphuric acid. The result of which, is waters with high sulphide concentrations (sulphuric acid), low pH (0-4), and a high level of varying heavy metals (dependent on the geology of the affected area). Lime neutralisation tanks are commonly used to treat AMD by mixing in slaked lime slurry to form metal hydroxides (heavy metal removal) whilst simultaneously raising the pH to levels suitable for discharge (6.5 to 8.5).

It is essential during neutralisation that the solution be uniformly mixed throughout the process, to achieve ideal reaction kinetics and the ability to predict discharge water qualities. An abandoned gold-copper open pit mine in Queensland uses lime neutralisation, however, the mixing tanks used on site show signs of inadequate mixing conditions that result in significant lime scaling. The morphology of the scale deposits show that at least three different mixing conditions exist in the current neutralisation tank.

A transient single phase model of a current tank design with a single square blade propeller was created in ANSYS, CFX 15.0. This simulation has assisted in the identification and understanding of the scaling potential and mixing behaviours that are present throughout the continuous treatment process.

INTRODUCTION

Acid mine drainage (AMD) is a type of wastewater that is often observed in mine sites, however, is most prominent in open pit mines that have been abandoned or closed (Johnson & Hallberg, 2005; Simate and Ndlovu, 2014). AMD occurs when deep layers of sulphide rich materials are exposed to oxygen and water which reacts to form sulphuric acid. Thus, when rain water pools in a mine site; it characteristically displays a high concentration of sulphide, salt, dissolved heavy metals, and a low pH (Simate and Ndlovu, 2014; Sánchez-Andrea et al, 2014). Acid generation consequently causes a progressive decrease in pH (e.g. pH <4), which in turn increases the solubility of sulphates and any metals that may be present in the sediment and neighbouring rocks (Taylor et al, 2005; Australian Department of Industry, Tourism and Resources, 2007). The exact composition of AMD is dependent on the geology of the effected site (Akcil, 2005).

All around the world, significant AMD cases at decommissioned mines are left to perpetuate as treatment technologies are labelled either too expensive or inadequate (Akcil, 2005, Unger, 2012).

AMD water levels can be controlled and mitigated with active lime neutralisation technology, essentially reducing the water level by treating it to return it to a safe, neutral quality and then releasing it into the surrounding environment (Johnson & Hallberg, 2005). Lime neutralisation is the most common and environmentally effective technique available for the treatment of AMD (Cripps, 2013; Taylor and Cox, 2003; Quast, 1996; Johnson & Hallberg, 2005; Akcil, 2005).

Lime neutralisation is a relatively simple technology, which involves the addition of slaked lime to AMD and a form of mechanical agitation (Johnson & Hallberg, 2005; Akcil, 2005). An effective form of mechanical agitation is essential to facilitate uniform mixing, maximise suspended reaction time, and prevent premature deposition. The presence of alkaline lime slurry, in turn precipitates metal hydroxide species, as the pH of the solution is raised to neutral values. Further downstream, the mixed solution enters a clarifier which removes impurities that have precipitated out of suspension before being discharged in the nearby river system. Although the lime neutralisation process is a relatively simple one, severe scaling is often present in the early stages of treatment, which is a major issue that requires frequent maintenance and plant shutdowns.

This investigation focusses on the flow patterns that facilitate the formation of different types of scale, which will provide useful data on how to minimise or control scaling in lime neutralisation tanks.

The following figure is a typical layout of an AMD neutralisation tank:

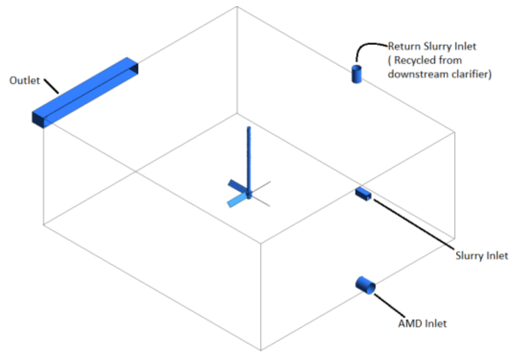

Figure 1: Typical AMD Neutralisation Tank Layout

LIME NEUTRALISATION TANK SCALING ISSUES

A site visit to a Queensland abandoned mine using lime neutralisation in September 2014 found that there were significant lime deposits on the walls, base and corner of the neutralisation tank. This is a common problem in most lime neutralisation tanks. Scaling is likely due to inadequate mixing conditions in the system and contributes to maintenance expenses and plant shutdowns. It is expected that the efficiency of such a treatment facility is dependent on uniform mixing at the first stage where the lime slurry and AMD are introduced (Vicum & Mazzotti, 2007; Bałdyga et al, 2005). For example, operating technicians have reported needing to introduce extra lime to account for the lime that is lost and deposited on the walls and base of the tank in stagnate areas. Without additional lime slurry, the output from the clarifier would likely not reach discharge qualities and would need to be recirculated back into the neutralisation tank to reduce pH levels further.

The morphology of the scale deposits can be observed in Figure 2 and ranged from;

Type A - Dense Layering, Sedimentary Scale: A dense layering of solids that resembles a sedimentary rock formation; located on the base and lower walls of the rectangular tank where lime slurry is introduced.

Type B - Ripple Wave Scale: A dense layering of solids that has a smooth surface and resembles a rippling wave; located on the upper walls of the tank where lime slurry is introduced.

Type C - Barnacle Scale: Small, smooth scale deposits that resemble barnacles; located on the outlet wall of the tank.

Type D - Rough Layered Scale from the Weir: A dense, rough layering of solids; located on the outlet weir.

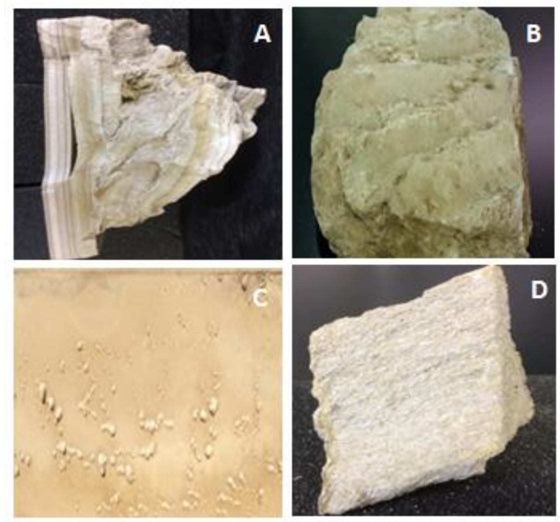

Figure 2: Types of Scale Deposits Identified

Experimentally identifying the flow characteristics that facilitate the formation of these scale types is difficult due to the opaque colour of the lime slurry and consequently the whole batch once the neutralisation tank reaches a steady state. Therefore, computational fluid dynamics for this application is highly advantageous.

CFX MODEL DESCRIPTION

Results for this paper were obtained using CFD Code 15.0. CFX was chosen for its availability and capacity to define multiple domains of both moving and stationary reference frames, in the same model.

In addition to the mechanically powered propeller, the neutralisation tank modelled is rectangular with concrete walls, containing three inlets and one outlet. The 0.9 meter mechanical propeller is located in the middle of the tank, one meter above the base, the remaining geometric details and the mass flow rates for each inlet are listed in Figure 3. To minimise solving time only one fluid material, water at 25 °C, was specified to enter from each of the inlets and the reaction kinetics were not simulated.

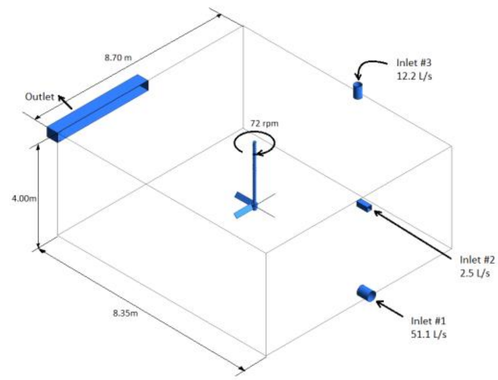

Figure 3: CFX Model Geometry

The numerical mesh consisted of just under 300,000 tetrahedral cells. Domains and regions of high mass flow rates, expected high velocities, and rotational speed, such as around the inlets, outlet and the rotating propeller domain were refined to facilitate accurate results. The model coordinate frame was also at the rotating propeller

To set up this single phase model transient analysis was specified with running time duration of 1800 seconds and a time step of 0.5 seconds, to be sure that a steady state was reached and that the flow at this point could be observed over a reasonable amount of time. A total of six fluid domains and interfaces were developed, this included the main domain of the tank, one for each of the inlets and outlet and another for the rotating propeller which was classified as an immersed solid. Longer inlet pipelines were used to allow a developed flow profile to cultivate from the plug flow that was specified.

The buoyancy and isothermal models were both activated to apply gravity to the mixing fluid and a uniform temperature respectively. Given the rotating domain of the propeller mesh deformation was permitted in regions of specified motion.

Applying the correct turbulence model to any CFX flow case is important. For fluid flow, the most commonly used and prominent turbulence model is k-epsilon. It has been proven to be stable, numerically robust and sufficiently accurate for a broad range of applications (Wilkening et al, 2008). In this case, the application of this model has produced results that are in good agreement with experimental and on-site data, in an efficient convergence time.

The boundary conditions of the wall are important for this case as the numerical flow patterns and velocities calculated will aid the explanation of why these types of scales are forming during operation. The No Slip Wall condition and stationary mesh motion were set, to avoid impeding flow predictions. The wall roughness was set to resemble a coarse concrete, to facilitate actual operating conditions.

Solid particles where not introduced to the model for this paper.

The validity of the numerical results from CFX has been confirmed by comparison to small scale experimental testing and data gathered on an additional site visit in July 2015. At this site visit the flow profile of the surface water was examined and the following was noted:

- A distinctive central line where two opposing flow momentums meet and velocity is dispersed.
- Small swirls developed along this central line and moved towards the main propeller whirlpool until they were consumed
- Slower fluid motion around the slurry inlet.
- Slurry enters the tank in frequent bursts caused by the speed and capacity of the pump, which transports the slurry in from external lower mixing reservoirs to up over the side of the walls.

This central line and an example of a small swirl are illustrated in Figure 4.

Figure 4: Small Swirls Observed on Site Visit at Central Line

Both the numerical results calculated by CFX 15.0 and the small scale physical experimental outcomes show a good agreement to the surface flow observed at the site visit. These results indicated:

- A central distinctive line where two opposing fluid momentums meet. The mechanism behind this trait is axial flow, due to the propeller forcing the fluid out towards the wall boundary which it follows up towards the surface and completes a full circle. This is clearly seen in Figure 5.
- Small swirls develop frequently along this line, on both sides of the propeller for a short period of time before they are absorbed by the momentum of the agitator. This is illustrated in Figures 5 and 6.
- Clearly identifiable regions of stagnant and low velocity fluid flow (corners, along inlet walls), and alternatively regions of comparatively faster fluid movement (outlet wall). This is again illustrated in Figures 5 and 6.

Numerical CFX Outcomes

Numerical outcomes are shown in Figure 5.

Physical Experimental Outcomes

Experimental testing showed strong similarities to the theoretically generated CFX results. Like Figure 5 a swirl develops in the same region before it was consumed by the higher velocity fluid around the propeller. Higher velocities were also observed along the outlet wall as the blue dye dissolved at a much greater rate in comparison to the walls with inlets.

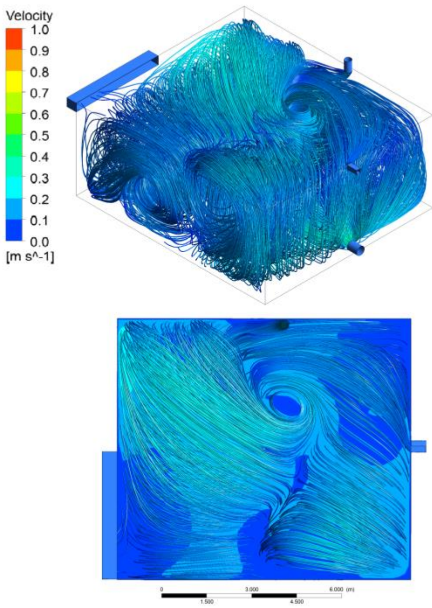

Figure 5: CFX Velocity Streamlines and Velocity Surface Contour at 850 seconds

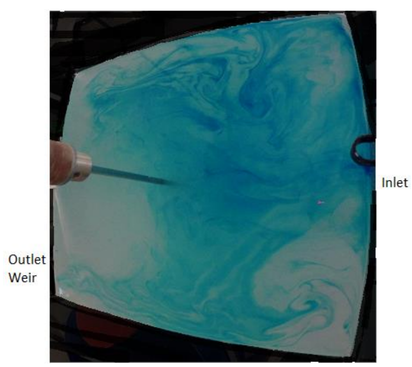

Figure 6: Surface Flow Patterns Observed During Experimental Confirmation

ANALYSIS

Bernoulli's principle states that a non-viscous, incompressible fluid pressure varies inversely with velocity. A decrease in fluid flow velocity produces an increase in pressure and vice versa (Marvin, 2012). Thus, it can be concluded that the static pressure along a streamline is highest when velocity is approaching zero (Arakeri, 2000), and ultimately in these areas of very low velocity and greater pressure, premature deposition is facilitated, as residence time is high. In this case pressure contours of the numerical results have been used to identify areas of likely deposition and scaling potential.

Figures 7 and 8 show that deposition is most likely to occur in the corners, along the lower walls and base of the tank. This can also be seen in Figure 5 where the velocity streamlines do not fully enter the corners.

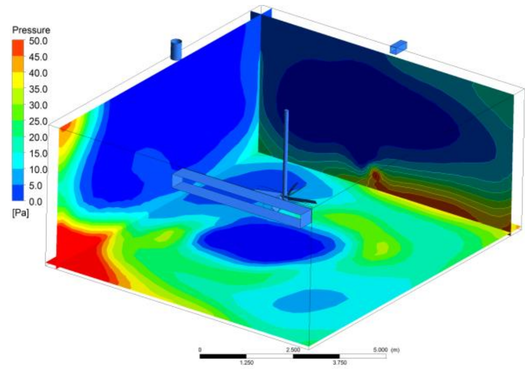

Figure 7: CFX Pressure Contours at 1000 Seconds

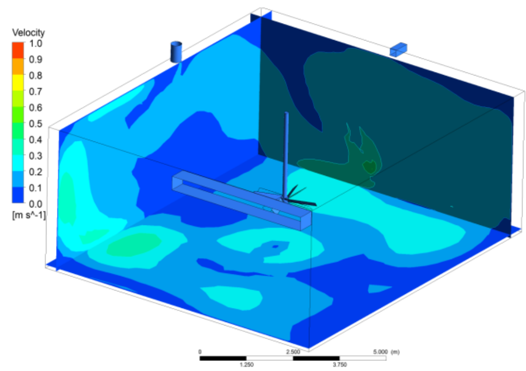

Figure 8: CFX Velocity Contours at 1000 seconds

IDENTIFYING SCALE FORMATION MECHANISMS

Scale Type A, the dense, layered sedimentary formation, appears to be caused by the slow deposition of lime particles in low velocity and near stagnant areas, Figure 7 and 8. Figure 9 shows that where residence time is high and the flow pattern is consistent in one direction, particle deposition becomes predictable in the early stages of operation.

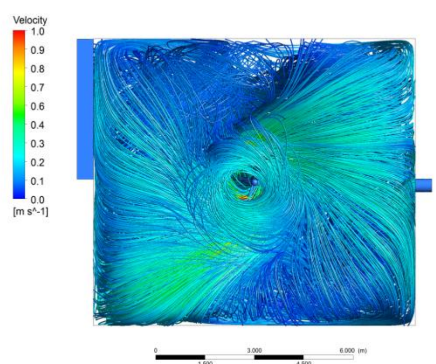

Figure 9: Constant Flow Profile on the Base of the Tank at 1000 Seconds

In Figure 2 it can be seen that the first 50 millimetres of deposition is uniform and after this point it becomes unpredictable. This is likely due to the fact that the scale after time fully occupies the stagnate area and starts too impeded on a more active flow regime, that is closer to the propeller mixing range.

The formation of Scale Type B, the dense, smooth ripple layering, is similar to Type A as they both occur in areas of lower velocity. However; Type 2 occurs in regions of higher particle counts, near the entries of the two dense lime slurry inlets (main and return), which enter in pulsating bursts of flow due to the speed and capacity of the pump. Therefore, as the mass flow rate of the slurry inlet is low in comparison, it is likely that the pulsating input governs the mixing regime along this wall, hence depositing in noticeable ridges.

Scale Type C, the barnacle scale, forms under vastly different flow conditions. This barnacle scale formation was observed on sections of the wall that experience a greater established velocity momentum as per numerical and experimental results. The small scale deposits are due to wall roughness and irregularities in the mean surface height. Each of the scale formations represent an obstacle on the surface of the wall that encourages the deposition by impeding the flow and ultimately preventing a particle from continuing along its path. Although this form of scaling is considerably less than the others identified, it has the potential to perpetuate and impede the flow substantially.

Scale type D, the dense rough layering on the outlet weir, has this pattern due to a constant flow pattern of the same direction at the same speed. The density and roughness of the scale sample suggests that the lime particles and impurities fall from suspension as soon as the flow is impeded or momentum is lost which further affirms that the current mixing system is not sufficient.

SUMMARY

A common lime neutralisation tank was modelled to aid in investigating the mixing mechanisms that occur within, and the relationship between mixing conditions and scale formation. Ultimately, CFX aided in identifying stagnant areas and the constant flow profiles that lead to the four different types of scales that typically form in AMD lime neutralisation tanks. It can be concluded that the rate, behaviour, and formation of lime scale deposition is dependent on the immediate flow patterns and mixing regimes that exist around areas of greater pressure and lower velocity.

RFERENCES

AKICL, A. (2005). "Acid Mine Drainage (AMD): causes, treatment and case studies." Journal of Cleaner Production **14**: 1139-1145.

ARAKERI, J. (2000). "Bernoulli's equation." Resonance **5**(8): 54-71.

AUSTRALIAN DEPARTMENT OF INDUSTRY, TOURISM AND RESOURCES (2007). Managing Acid and Metallferious Drainage. Leading Practice Sustainable Development Program For the Mining Industry. Australia, Department of Industry Tourism and Resources. **1:** 91.

BAŁDYGA, J. and Ł. MAKOWSKI (2004). "CFD Modelling of Mixing Effects on the Course of Parallel Chemical Reactions Carried out in a Stirred Tank." Chemical Engineering & Technology **27**(3): 225-231.

CRIPPS, A (2013). "Australia : Controlled water release at Mount Morgan Mine site." MENA Report.

JOHNSON, D. B. and K. B. HALLBERG (2005). "Acid mine drainage remediation options: a review." Science of The Total Environment **338**(1–2): 3-14.

MARVIN, S. (2012). Dictionary of Scientific Principles. Hoboken, Wiley**:** 647.

QUAST, K. B. Neutralisation of Acid Mine Drainage from Brukunga Pyrites Mine, Barton, ACT, Institution of Engineers, Australia.

SÁNCHEZ-ANDREA, I., J. L. SANZ, M. F. M. BIJMANS AND A. J. M. STAMS (2014). "Sulfate reduction at low pH to remediate acid mine drainage." Journal of Hazardous Materials **269**(0): 98-109.

SIMATE, G. S. and S. NDLOVU (2014). "Acid mine drainage: Challenges and opportunities." Journal of Environmental Chemical Engineering **2**(3): 1785-1803.

TAYLOR, G. F. and R. C. COX (2003). The Brukunga Pyrite Mine — A Field Laboratory for Acid Rock Drainage Studies. Sixth International Conference on Acid Rock Drainage (ICARD). Cairns, Australia, AusIMM. **6:** 93-106.

TAYLOR, J., S. PAPE and N. MURPHY (2005). A Summary of Passive and Active Treatment Technologies for Acid and Metalliferous Drainage (AMD) Fifth Australian Workshop on Acid Drainage. Fremantle, Western Australia, Australia Centre for Minerals Extension and Research (ACMER).

UNGER, C. (2012). Annex to The AusIMM Abandoned Mines policy statement Abandoned Mines: an overview of current status and AusIMM members' perspectives AusIMM Sustainability Committee 1-8.

VICUM, L. and M. MAZZOTTI (2007). "Multi-scale modeling of a mixing-precipitation process in a semibatch stirred tank." Chemical Engineering Science **62**(13): 3513-3527.

WILKENING, H., D. BARALDI and M. HEITSCH (2008). "CFD simulations of light gas release and mixing in the Battelle Model-Containment with CFX." Nuclear Engineering and Design **238**(3): 618-626.